



Optimization of Chitosan Concentration on Physicochemical Properties of Polyvinyl Alcohol-Based Hydrogel

Muhammad Saupi Azuri¹, Md. Shaekh Forid¹, Wan Maznah Wan Ishak¹, Nurul Ain Athirah Azhar¹

¹*Faculty of Chemical and Process Engineering Technology, University Malaysia Pahang Al-Sultan Abdullah, 26300 Gambang, Pahang, Malaysia.*

Abstract

Hydrogels are an interconnected three-dimensional polymeric network that are widely applicable for drug delivery, wound healing, tissue engineering and other biomedical uses. Recently, chitosan/polyvinyl alcohol hydrogels have been investigated for use as drug delivery carriers due to their ability to encapsulate, carry and release the drug to the intended target. For this purpose, the study was designed to fabricate a chitosan/ polyvinyl alcohol hydrogel and optimize the chitosan concentration in the hydrogel. To fabricate the chitosan/ polyvinyl alcohol hydrogel, chitosan at concentrations of 1.5%, 2.0%, 2.5%, and 3.0% were used and the polyvinyl alcohol concentration was fixed at 2.0% for each formulation. The chitosan/ polyvinyl alcohol hydrogels were investigated on their physicochemical properties, which were swelling rate, water vapour transmission rate, porosity and mechanical properties including tensile strength and elongation at break. Furthermore, the prepared hydrogels were characterized for functional properties using fourier-transform infrared spectroscopy and scanning electron microscope. The results showed that 1.5% chitosan/ polyvinyl alcohol hydrogel had the best physicochemical properties among the tested formulations. FTIR results for all formulations meet the criteria. The surface morphology of 1.5% chitosan/ polyvinyl alcohol hydrogel showed a porous structure. The results suggest that 1.5% chitosan/ polyvinyl alcohol hydrogel could be suitable for biomedical and pharmaceutical applications.

Keywords: chitosan, polyvinyl alcohol, hydrogel, optimization, physicochemical properties

Full length article *Corresponding Author, e-mail: wanzmah@ump.edu.my

1. Introduction

The hydrogel is known as 3D network structure consisting of hydrophilic polymeric chains that are crosslinked physically, chemically or via polymerization and known to hold abundant fluid within its polymeric chain networks from the surface tension and capillary forces during a swollen state [1]. Hydrogels have been commonly used in diversified fields such as biomedical, biomaterials, agriculture and food industry applications [2]. The use of hydrogels in the biomedical application is expanding, especially in the areas of targeted drug delivery [3,4], tissue regeneration [5] and wound healing [6,7]. Hydrogels exhibit promising properties in terms of their biodegradability, biocompatibility, absorption capacity and mechanical tunability. Nonetheless, the material and production method affect their properties [8]. Hydrogels are classified as natural or synthetic based on the materials used in their fabrication [9]. Fabrication of natural hydrogels based on chitosan appears to be a promising avenue of research. Chitosan is a

linear polysaccharide found in the exoskeleton of crustaceans, algae, insect cuticles, and fungal cell walls [10]. This material is highly biodegradable and biocompatible, making it an ideal choice for biomedical applications [11]. It has been discovered that chitosan hydrogels accelerate wound healing by inhibiting bacterial growth and enhancing hemostasis [12]. Research has demonstrated that it possesses excellent antioxidant and anti-inflammatory properties that promote wound healing [13]. One study showed that wound exudate was efficiently absorbed while maintaining wound surface moisture [14]. Additionally, a chitosan hydrogel was fabricated into bio-ink for artificial tissue and organ reconstruction and improved cell viability [15]. Despite these benefits, chitosan hydrogels have relatively poor mechanical strength due to their hydrophilic nature [16,17]. As such, a stronger hydrogel can be developed by blending chitosan with a synthetic polymer. Recent studies showed that chitosan is highly compatible with polyvinyl alcohol (PVA) to produce a robust hydrogel via physical crosslinking. PVA is a synthetic polymer that is soluble in water and biocompatible

[18] that can form a hydrogel through physical crosslinking, such as via the freeze-thawing technique due to its high number of hydroxyl groups and polymer crystallization [19]. This hydrogel is formed via repeated freeze-thaw cycles, without requiring an external crosslinking agent. The result is an ultra-pure, highly biocompatible hydrogel. PVA hydrogels also can be tailored to specific biocompatibility and properties by blending with a second polymer and/or nanoparticles, resulting in interpenetrating polymer networks and nanocomposite hydrogels. This allows for the fabrication of various materials such as prosthetics, drug delivery vehicles, and wound dressings. [20].

The use of chitosan and PVA together as composite materials has shown significant advancements. By encouraging angiogenesis and collagen deposition, arginine-modified chitosan/PVA hydrogel-based microneedles for sustained curcumin delivery have been demonstrated to hasten wound healing [21–23]. Jafari and Namazi (2023) [24] stated that a pH-responsive hydrogel could be potentially used for controlled delivery of curcumin for cancer therapy. Researchers have demonstrated that the hydrogel can sustainably control drug release in an in-vitro and in-silico study [25]. However, there are variances and inconsistencies in the formulation of these hydrogels. No studies have been conducted to optimize the chitosan concentration for use with PVA, particularly when employing the freeze-thaw technique as a physical crosslinking approach. Therefore, this study aimed to optimize the concentration of chitosan to achieve the best physicochemical and mechanical properties of the chitosan/PVA hydrogel. In this study, chitosan and PVA were mixed to prepare the chitosan/PVA hydrogel using different concentrations of chitosan while PVA concentration was fixed at 2% for each formulation. The hydrogels were characterized by measuring their swelling rate, water vapor transmission rate, and porosity. Tensile strength and elongation at break were used as metrics to determine the impact of chitosan concentrations on the mechanical properties of hydrogels. Finally, fourier transform infrared spectroscopy (FTIR) and scanning electron microscopy (SEM) were employed to validate the hydrogels' functional group and surface morphology.

2. Materials and methods

2.1 Materials

PVA (85,000-124,000 g/mol-1, 99% hydrolyzed) and phosphate buffered saline (PBS, pH 7.4) were purchased from Sigma-Aldrich (USA). Ethanol was purchased from R&M Chemical (Malaysia). Collagen extracted from Pangasianodon hypophthalmus skin which was collected from a local fish farm in Pahang, Malaysia. Chitosan was purchased from Natherm Group Sdn Bhd (Malaysia).

2.2 Hydrogel preparation

Initially, chitosan was dissolved in deionized water to produce a chitosan stock solution of 10% (w/v). The PVA stock solution of 10% (w/v) was also prepared by dissolving PVA granules in deionized water that was preheated to 60°C. Under vigorous stirring, the temperature was gradually increased to 90°C until the PVA was fully dissolved. Then, Azuri et al., 2023

the chitosan/PVA hydrogel was prepared by mixing the chitosan stock solution and PVA stock solution. These stock solutions were mixed at different ratios under vigorous stirring for 10 min until a homogenous solution was formed (Table 1). The solutions were then poured into petri dishes. Then, the solutions were frozen at -4°C for 12 h and thawed at room temperature for 4 h. This freeze-thaw process was repeated for 3 cycles until the hydrogels were formed. Finally, the hydrogels were lyophilized using a freeze-dryer. This process is summarized in Fig 1.

2.3 Characterization of hydrogels

2.3.1 Swelling rate

Initially, the initial dry weight of the hydrogel was recorded. Then, the hydrogel was immersed in PBS solution at 37°C for 24 h. After soaking, the hydrogel was removed from the PBS solution and blotted dry. The weight of the hydrogel was measured at specific time intervals. The swelling ratio was calculated according to the following Equation 1:

$$\text{Swelling ratio (\%)} = (W_s - W_d) / W_d \times 100 \quad (E1)$$

Where W_s and W_d are the weight after swelling at the specific time intervals and the dry weight of the hydrogel, respectively. All measurements were repeated three times ($n = 3$).

2.3.2 Water vapour transmission rate (WVTR)

The moisture permeability of the chitosan/PVA hydrogels were determined by measuring the water vapor transmission rate (WVTR). Briefly, the chitosan/PVA hydrogels were cut to a diameter of 25 mm and placed at the mouth of a centrifuge tube that contained 8 ml of deionized water. Parafilm was used to seal the gap between the hydrogel and the centrifuge tube to avoid gas leakage. The area of the exposed hydrogel surface and the initial weight of the centrifuge tube containing hydrogel was measured (W_i). These centrifuge tubes were then placed in the incubator at 37°C with a humidity of 70 %. The weight of the centrifuge tube with the hydrogels were then measured at specific time intervals (W_f). WVTR was calculated according to the following Equation 2:

$$\text{WVTR (g/m}^2\text{/h)} = ((W_f - W_i)) / (A \times H) \quad (E2)$$

Where W_i and W_f are the initial and final weight of the centrifuge tube with hydrogel, respectively. A is the area of the exposed hydrogel surface (m^2). H is the specific time interval. All measurements were repeated three times ($n = 3$).

2.3.3 Porosity

The porosities of the prepared chitosan/PVA hydrogels were measured by solvent replacement method. Briefly, the hydrogels were cut, and their volume and weight were measured. Then, the chitosan/PVA hydrogels were immersed in an absolute ethanol for 2 h at 37°C in a sonicator bath. The samples were taken out and the final weight of hydrogels were recorded. The porosity was calculated according to Equation 3:

$$\text{Porosity (\%)} = (W_f - W_i) / (\rho V_1) \times 100 \quad (\text{E3})$$

Where W_i and W_f are the initial and final weight of the hydrogel respectively. V_1 represents the volume of the sample and ρ is the density of absolute ethanol (0.79 gml⁻¹) at room temperature. All measurements were replicated three times ($n = 3$).

2.3.4 Mechanical property test

The tensile strength (TS) and elongation at break (EB) of the hydrogel were measured using a Universal Tensile Machine at room temperature. Firstly, the hydrogel's length, width and thickness were recorded. Then, the hydrogels were firmly fixed to the jaws of the tensile tester. The tensile strength of the membranes was measured with an extension speed of 20 mm/min until breaking. The TS and EB were calculated according to the Equation 4 and 5:

$$\text{Tensile Strength (MPa)} = F_b / (T \times W) \quad (\text{E4})$$

$$\text{Elongation (\%)} = D/L \times 100 \% \quad (\text{E5})$$

Where F_b represents the maximum force (N) of the sample during tensile fracture. D represents the elongation of the samples at break, and T , W and L are the thickness, width and length of the samples. All measurements were repeated three times ($n = 3$).

2.3.5 ATR-FTIR analysis

Attenuated total reflectance-Fourier Transform Infrared Spectroscopy (ATR-FTIR, Shimadzu Corporation, Japan) was used to identify the presence of chemical bond of the chitosan/PVA hydrogel. A hydrogel sample was placed onto the crystal cell and mounted. The spectra were recorded in transmission mode with a resolution of 4 cm⁻¹ in the range of 4000-400 cm⁻¹ at room temperature.

2.3.6 Scanning electron microscope

The interior structure of the collagen/PVA hydrogels were observed with a SEM (Hitachi TM3030 Plus, Japan). The samples were freeze-dried and then cut into halves. Then, the hydrogel was mounted on aluminium studs and coated with gold prior to examination. The SEM images of the interior surface were taken with magnification of 100x and 500x.

2.4 Statistical analysis

All quantitative data were presented as a mean \pm standard deviation (SD). GraphPad Prism version 5.0 (GraphPad Software, Inc) was used for statistical analysis. P values of less than 0.05 ($P \leq 0.05$) were considered significant. Statistical analyses of the data were performed by one-way analysis of variance (ANOVA).

3. Result and Discussion

3.1 Swelling rate

Hydrogels can absorb a considerable amount of aqueous solution and store it in an aqueous environment
Azuri et al., 2023

within the polymer matrix that causes it to swell [26]. The water-absorbing ability and swelling behavior of polymeric hydrogels are influenced by their composition, degree of crosslinking, and external factors such as temperature and pH [27]. The optimal concentration of chitosan was determined by studying the swelling behavior of chitosan/PVA hydrogel and evaluating their water uptake capacity. Fig 2 shows the swelling rate of chitosan/PVA hydrogel determined by measuring their weight changes after soaking in PBS. After 24 hours, the swelling rates of chitosan/PVA hydrogels with concentrations of 1.5%, 2.0%, 2.5%, and 3.0% were $337.82 \pm 1.98\%$, $581.70 \pm 31.13\%$, $600.00 \pm 41.33\%$, and $517.34 \pm 10.03\%$, respectively. The swelling rates were not significantly different from each other. According to the finding from FTIR (Fig 8), the main functional groups in these hydrogels were -NH and -OH group, which are hydrophilic. Initially, the -NH₂ functional group of chitosan is protonated to -NH₃⁺ and forms a bond with a water molecule. The -OH group could also easily form a hydrogen bond with water molecules [28,29]. These actions cause the hydrogels to swell due to diffusion of water molecules. Moreover, increasing concentration of chitosan in the hydrogel will increase the density of the -NH₃⁺ and -OH group, thus higher swelling rates were recorded for the 2.0% to 3.0% chitosan/PVA hydrogels compared to the 1.5% chitosan/PVA hydrogel. A similar finding was reported by Chopra et al. (2022) [25] in which the swelling ratio of water increased as the concentration of chitosan increased in the hydrogel.

3.2 Water vapour transmission rate (WVTR)

WVTR directly controls the moist microenvironment of wound healing. WVTR can be used to assess the capacity of a wound dressing in preventing the water loss. The moisture of a wound surface can be controlled by applying different wound dressings with specific WVTR. A wound might be dehydrated by a very high WVTR, whereas a very low WVTR wound may cause exudates [30]. The chitosan/PVA hydrogel at 2% produced the highest WVTR (Fig 3). Increasing the chitosan concentration resulted in a reduction of WVTR as shown by the 2% chitosan/PVA hydrogel that had a WVTR of 883.18 ± 16.16 g/m²/day compared to the 3% chitosan/PVA hydrogel with only 711.43 ± 33.24 g/m²/day. When the chitosan concentration is increased, the availability of free hydrophilic functional groups of chitosan such as -NH₃⁺ and -OH also increases. These functional groups formed a stronger bond with water molecules, thus preventing the water from evaporating [31]. In contrast, a 1.5% chitosan/PVA hydrogel showed a significantly reduced WVTR. Due to a lower concentration of chitosan used in the 1.5% hydrogel in comparison to the PVA, there is less hydrogen bond-induced polymeric crosslinking between chitosan and PVA, which increases the free availability of -OH bonds from PVA. Water will bind to a free -OH bond, preventing water loss by evaporation. This result suggests that the concentration of available hydrophilic functional groups, such as -NH and -OH in the hydrogel was the factor influencing the WVTR of chitosan/PVA hydrogel.

3.3 Porosity analysis

Porosity refers to the proportion of empty space in a material, which depends on the organization of the polymer network during the sol-gel transition, the conditions under which it is crosslinked, and the concentration of the polymer present [32]. Fig 4 shows the porosity of different formulations of chitosan/PVA hydrogels in the range of 44.90-66.6%. The 1.5% chitosan/PVA hydrogel was more porous at $66.6 \pm 18.64\%$, but was not significantly different compared to 2.0% ($59.01 \pm 15.23\%$), 2.5% ($55.91 \pm 17.14\%$) and 3.0% ($44.90 \pm 6.95\%$) chitosan/PVA hydrogels. Hydrogels with more than 60% porosity can effectively promote bone regeneration in vivo and cell proliferation and osteogenic differentiation in vitro [33]. Similarly, hydrogels with a porosity of about 50% are favourable for cellular metabolism and nutrient exchange. [34]. Our finding is consistent with previous reports that the porosity in the structure of chitosan/PVA hydrogel decreased with an increase of chitosan concentration [35]. The concentration of polymer is the primary causal of porosity reduction. As the concentration of chitosan increased, the number of intermolecular crosslinks per primary molecules will also increase, thus reducing the total porosity [36]. The other causative factors are the implementation of repeated freeze-thaw cycle and freeze drying. The formation of diluted polymer-lean and concentrated polymer-rich phases increases with repeated freeze-thaw cycles. The pores are formed by the polymer-lean phase while polymer-rich phase will create the internal structure of the hydrogel. Furthermore, the rapid cooling used in the freeze-drying process resulted in a thermodynamic instability that caused a phase separation. Sublimation eliminates freezing solvent, leaving voids in the previously occupied regions.

3.4 Mechanical properties

One of the most significant parameters for wound dressings is the mechanical properties of the hydrogel. Tensile testing is used to evaluate the mechanical characteristics of hydrogels. Hydrogels are close to the skin's surface when used as a wound dressing. It should be resistant to tearing when stretched out to its maximum length. The tensile strength and percentage of elongation at break of chitosan/PVA hydrogels are shown in Fig 5 and Fig 6. The results indicated that the tensile strengths were not significantly different between all the hydrogels, which were between 0.179 ± 0.047 to 0.214 ± 0.033 MPa. The chitosan/PVA hydrogels exhibited a strain hardening during deformation, which was mainly attributed to the crystalline structure of the PVA polymeric network [37]. The strain hardening was observed when the polymeric chains of PVA between the crystalline structure demonstrated a finite extensibility to afford deformation. When the deformation reached a maximum extension, the crystalline structure slipped and the polymeric chain broke, which introduced a crack and caused a rapid fracture of the hydrogel. The tensile strength behavior of the polymer hydrogels did not exhibit a significant trend as it was influenced by several factors such

as changes in crosslinking and polymerization process, swelling conditions and mechanical anisotropy of the materials [38]. Meanwhile, the elongation at break is directly proportional to the concentration of the chitosan. The 3.0% chitosan/PVA hydrogel exhibited the greatest elongation at break measuring $231.960 \pm 20.897\%$ without significantly differentiating from other hydrogels. Adding the chitosan into the hydrogel formulation enhanced the formation of varying sized pores and disturbed the hydrogel's stable three-dimensional polymer network, which lowered the network densities in the hydrogel [39]. The polymeric interaction also dramatically weakened as the porosity was larger than that of the PVA hydrogel [40]. The loose interpolymeric structure of the hydrogel gives it greater flexibility and elasticity when it stretches during deformation. Both chitosan and PVA polymeric networks synergistically played an important role in maintaining the structural integrity of the hydrogel. The external force during tensile testing caused the molecular structure of the hydrogel to deform. It has been demonstrated that the chitosan polymeric network absorbs a significant amount of fracture energy during deformation, while PVA retains the shape of the hydrogel [41,42].

3.5 Fourier Transform Infrared Spectroscopy (FTIR) analysis.

FTIR spectrometry was used to determine the chemical structure of the chitosan/PVA hydrogels. The spectra of the chitosan/PVA hydrogels are shown in Fig 7 while Fig 8 shows the spectrum characteristics of both PVA and chitosan. All chitosan/PVA hydrogels exhibited similar 3 major peaks. The peak at 3317 cm^{-1} corresponds to the vibration of the N-H group of chitosan and the combination of the -OH group of chitosan and PVA. The peak at 1636 cm^{-1} is related to the association of water in the hydrogel [43]. The vibration of C-O stretching that overlaps between chitosan and PVA was observed at 1080 cm^{-1} [44]. A broad band at 3317 cm^{-1} indicated the presence of the hydroxyl group which may be related to the crosslinking hydrogel bonds between chitosan and PVA polymers.

3.6. SEM morphology analysis

The cross-sectional morphology and microstructure of chitosan/PVA hydrogel was observed using SEM at magnification of x100 and x500. As 1.5% chitosan/PVA showed the best physicochemical and mechanical properties among other formulations, therefore it was selected for SEM analysis. A 1.5% chitosan/PVA hydrogel exhibited an irregular pore size with the average size of $32.25 \pm 2.28\text{ }\mu\text{m}$ as illustrated in Fig 9. For skin recovery purpose, the ideal average pore size of the hydrogel should be in the range of $20\text{ }\mu\text{m}$ to $120\text{ }\mu\text{m}$ [45]. A proper pore size could control drug loading and drug release while absorbing wound exudate. The micropores in the hydrogel were also interconnected and evenly distributed, which facilitate the diffusion of oxygen and nutrient [46].

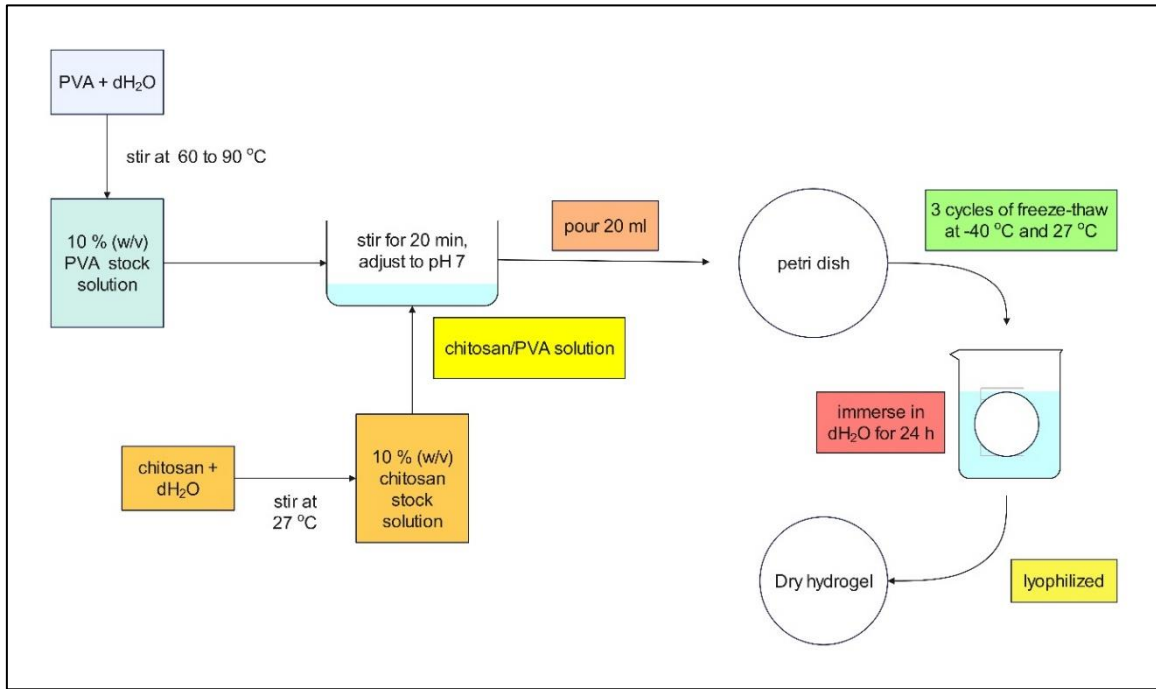


Fig 1. Schematic illustration of the chitosan/PVA hydrogel preparation.

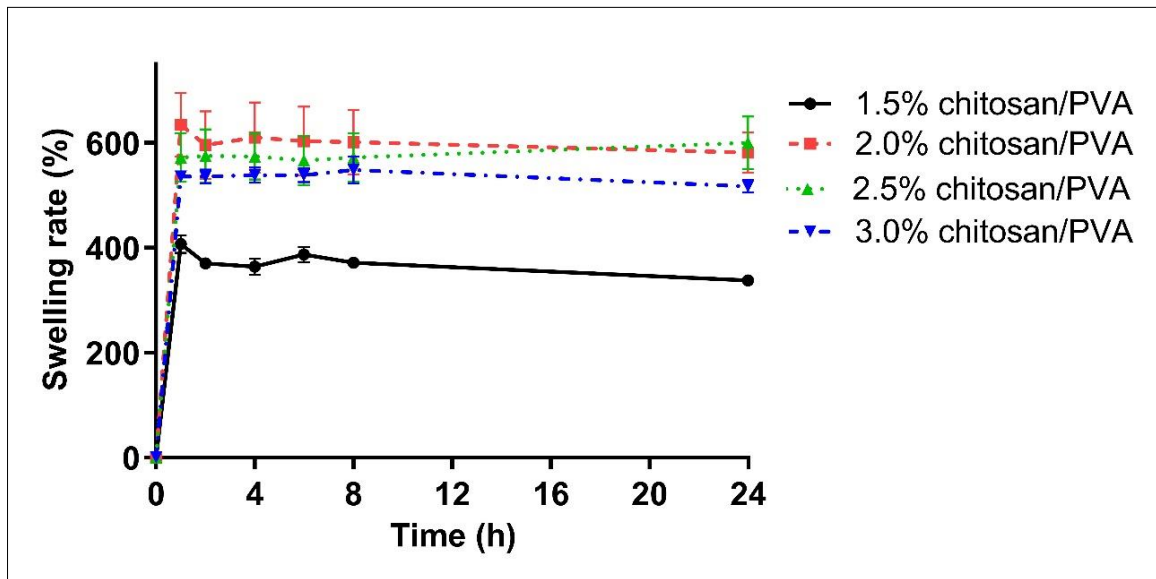


Fig 2. Swelling rate of chitosan/PVA hydrogel at different concentrations of chitosan while 2.0% PVA concentration was kept constant.

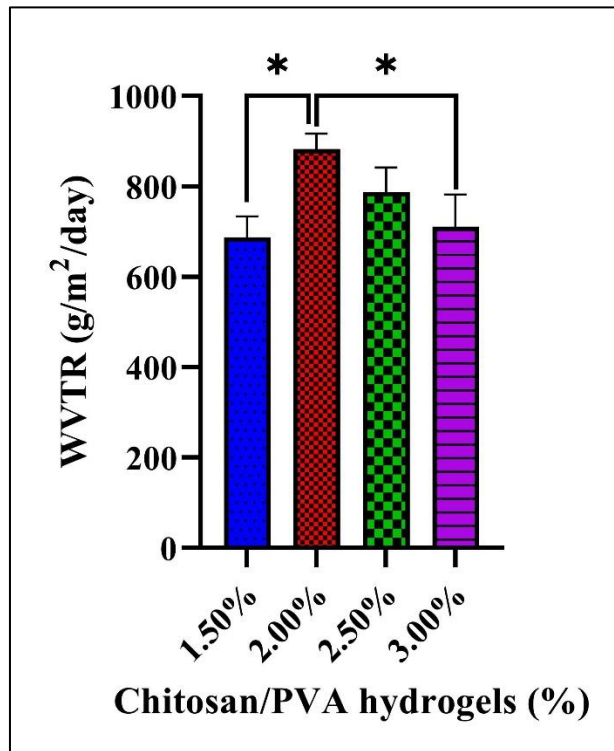


Fig 3. WVTR of chitosan/PVA hydrogels.

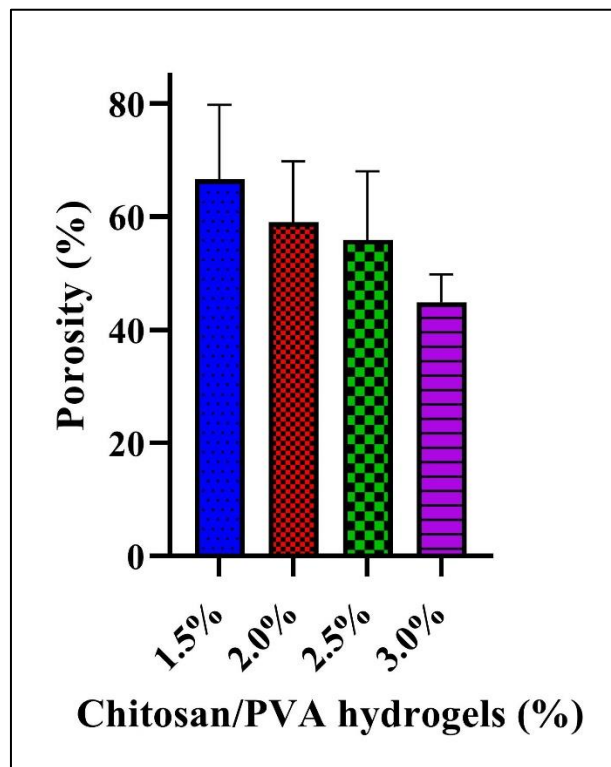


Fig 4. Porosity of the chitosan/PVA hydrogels.

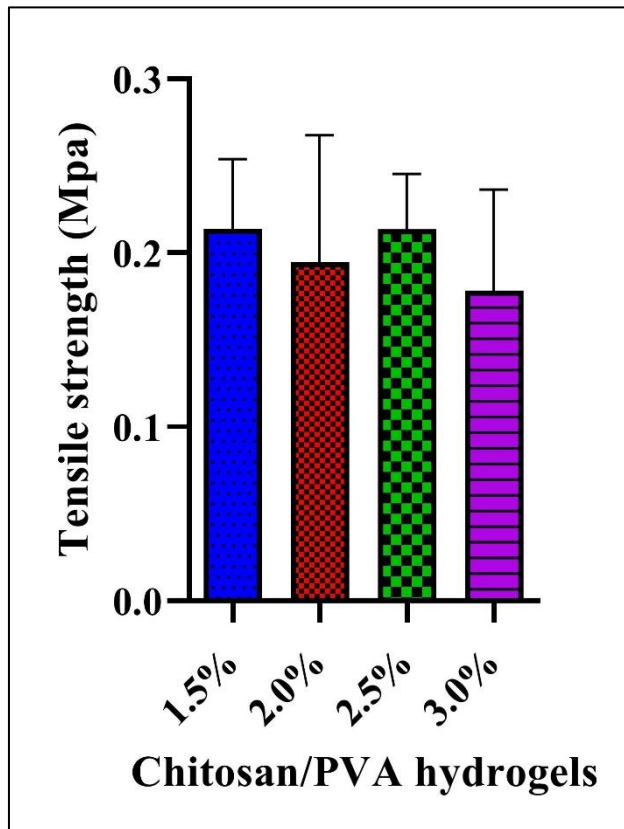


Fig 5. Tensile strength of the chitosan/PVA hydrogels.

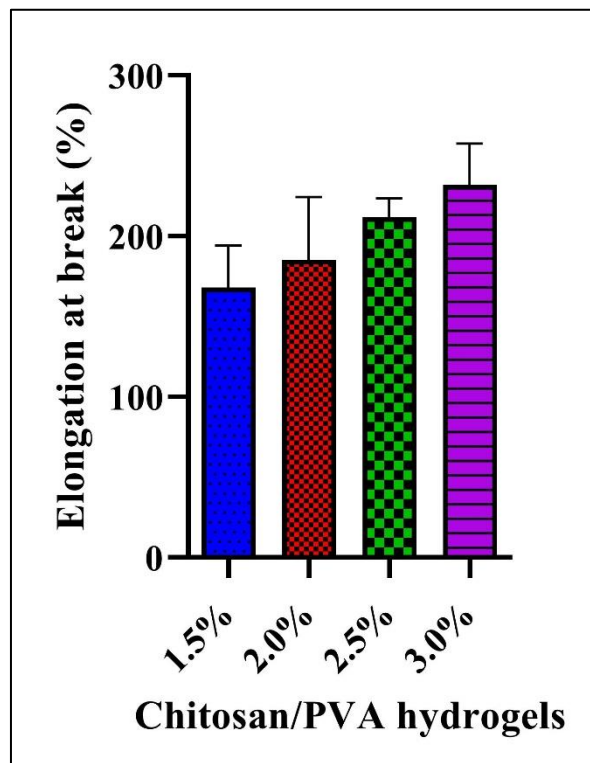


Fig 6. Elongation at break of the chitosan/PVA hydrogels.

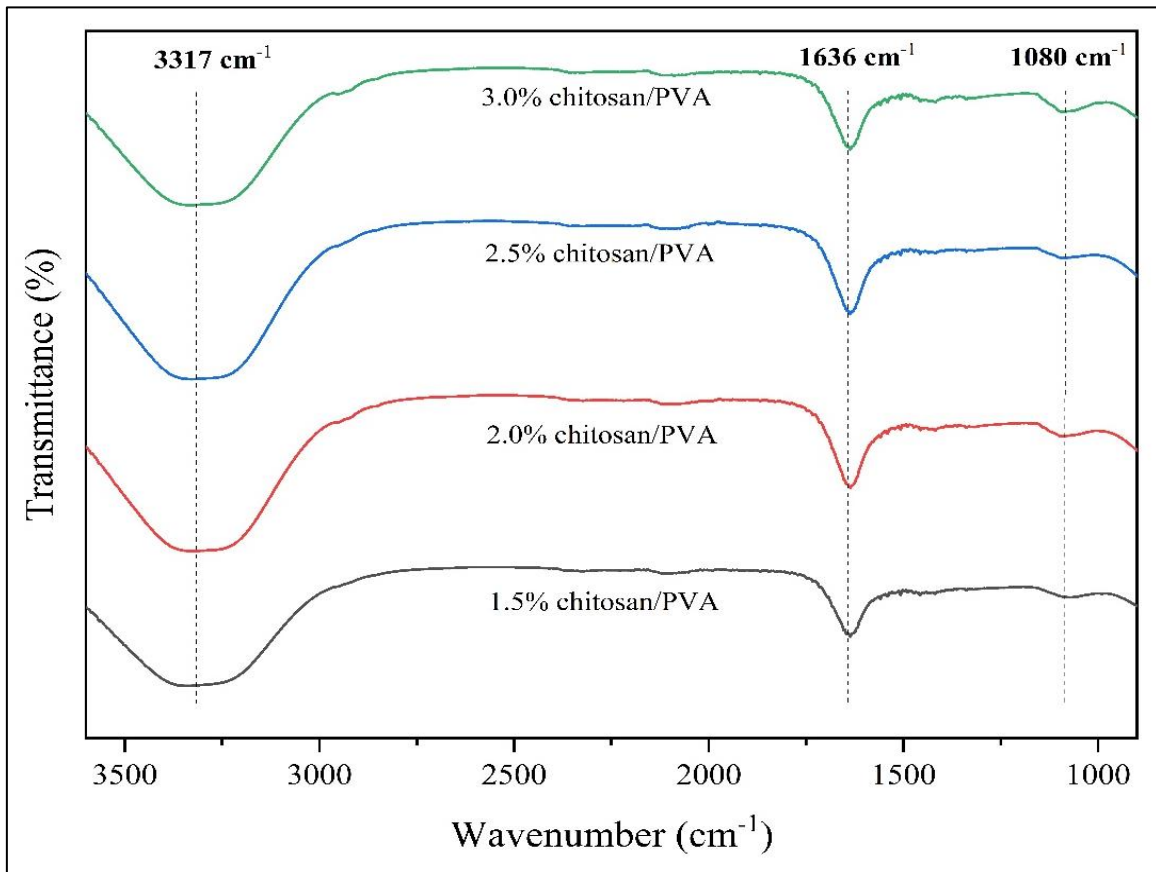


Fig 7. FTIR spectra of chitosan/PVA hydrogels.

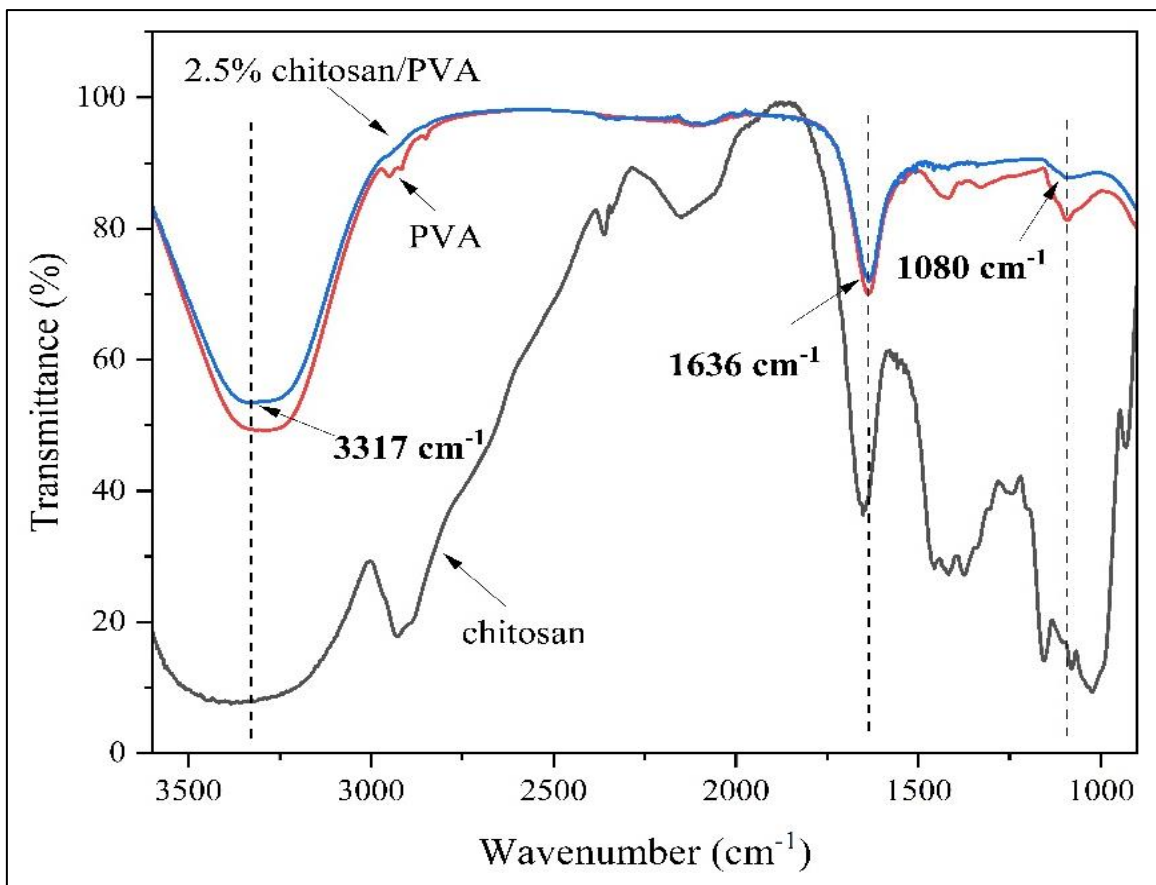


Fig 8. FTIR spectra of chitosan/PVA hydrogel, single PVA and single chitosan.

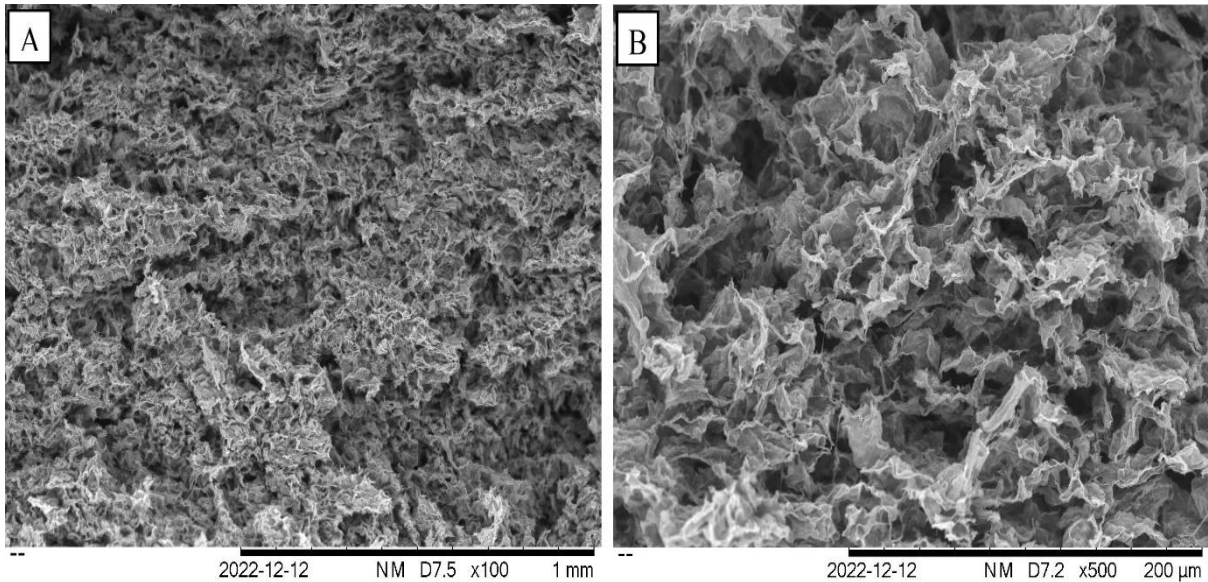


Fig 9. SEM micrographs of 1.5% chitosan/PVA hydrogel where (a) magnification $\times 100$, (b) magnification $\times 500$

Table 1 Formulation of Chitosan/PVA hydrogels.

Chitosan stock (ml)	Chitosan final concentration (%)	PVA stock (ml)	PVA final concentration (%)	Deionized water (ml)	Total volume of hydrogel (ml)
3.0	1.5	4.0	2.0	qs	20
4.0	2.0	4.0	2.0	qs	20
5.0	2.5	4.0	2.0	qs	20
6.0	3.0	4.0	2.0	qs	20

Table 2 Mechanical properties of the hydrogels.

Hydrogel	Tensile Strength (Mpa)	Elongation at Break (%)
1.5% chitosan/PVA	0.214 \pm 0.033	168.204 \pm 21.251
2.0% chitosan/PVA	0.195 \pm 0.060	185.468 \pm 31.685
2.5% chitosan/PVA	0.214 \pm 0.026	211.804 \pm 9.621
3.0% chitosan/PVA	0.179 \pm 0.047	231.960 \pm 20.897

Values are represented as mean \pm S.E.M, where (n = 3).

4. Conclusions

The purpose of this study is to determine the optimum concentration of chitosan that produced good physicochemical properties of hydrogel. Fabrication of hydrogels were made using various chitosan concentrations ranging from 1.5% to 3.0% while fixing the PVA concentration at 2.0%. Though not significant, 2.5% chitosan/PVA hydrogel swelled more than the other formulations. On the other hand, 1.5% chitosan/PVA hydrogel exhibited greater porosity and it was consistent with SEM observation indicating that the porosity increased as concentration of chitosan decreased. Likewise, 1.5% chitosan/PVA hydrogel also produced stronger mechanical properties as opposed to other tested formulations. FTIR analysis revealed the presence of three major functional groups of chitosan and PVA in all hydrogel formulations. In conclusion, the hydrogel with a chitosan concentration of 1.5% in 2.0% PVA demonstrated good physicochemical

Azuri et al., 2023

characteristics and is comparable with commercially available hydrogel wound dressings. Therefore, it is plausible that 1.5% could be the ideal chitosan concentration to formulate in hydrogels for future biomedical and pharmaceutical applications.

Acknowledgment

The work is funded by University Malaysia Pahang (UMP) AI-Sultan Abdullah under the grant number RDU200305 and PGRS210312. The authors acknowledge the assistance from the Faculty of Chemical and Process Engineering Technology (FTKPP), UMPSA for providing the equipment and facilities to carry out this research.

Conflict of Interest

The authors affirm no conflict of interest and take full responsibility for the paper's content.

References

- [1] S. H. Zainal, N. H. Mohd, N. Suhaili, F. H. Anuar, A. M. Lazim, and R. Othaman (2021). Preparation of cellulose-based hydrogel: a review. *J. Mater. Res. Technol.*, 10, 935–52.
- [2] T-C. Ho, C-C. Chang, H-P. Chan, T-W. Chung, C-W. Shu, K-P. Chuang, T-H. Duh, M-H. Yang, and Y-C. Tyan (2022). Hydrogels: Properties and Applications in Biomedicine. *Molecules*, 27, 2902.
- [3] J. Ma, D. Guo, X. Ji, Y. Zhou, C. Liu, Q. Li, J. Zhang, C. Fan, and H. Song (2023). Composite Hydrogel for Spatiotemporal Lipid Intervention of Tumor Milieu. *Adv. Mater.*, 35, 2211579.
- [4] H. Zhang, S. Wu, W. Chen, Y. Hu, Z. Geng, and J. Su (2023). Bone/cartilage targeted hydrogel: Strategies and applications. *Bioact. Mater.*, 23, 156–69.
- [5] J. Guo, H. Yao, X. Li, L. Chang, Z. Wang, W. Zhu, Y. Su, L. Qin, and J. Xu (2023). Advanced Hydrogel systems for mandibular reconstruction. *Bioact. Mater.*, 21, 175–93.
- [6] F. A. Farazin, Shirazi, and M. Shafiei (2023). Natural biomarocmolecule-based antimicrobial hydrogel for rapid wound healing: A review. *Int. J. Biol. Macromol.*, 244, 125454.
- [7] T. Wang, W. Yi, Y. Zhang, H. Wu, H. Fan, J. Zhao, and S. Wang (2023). Sodium alginate hydrogel containing platelet-rich plasma for wound healing. *Colloids Surf. B Biointerfaces*, 222, 113096.
- [8] P. Sánchez-Cid, M. Jiménez-Rosado, A. Romero, and V. Pérez-Puyana (2022). Novel Trends in Hydrogel Development for Biomedical Applications: A Review. *Polymers*, 14, 3023.
- [9] H. Cao, L. Duan, Y. Zhang, J. Cao, and K. Zhang (2021). Current hydrogel advances in physicochemical and biological response-driven biomedical application diversity. *Signal Transduct. Target. Ther.*, 6, 1–31.
- [10] Aranaz, A. R. Alcántara, M. C. Civera, C. Arias, B. Elorza, A. Heras Caballero, and N. Acosta (2021). Chitosan: An Overview of Its Properties and Applications. *Polymers*, 13, 3256.
- [11] R. Ye, S. Liu, W. Zhu, Y. Li, L. Huang, G. Zhang, and Y. Zhang (2023). Synthesis, Characterization, Properties, and Biomedical Application of Chitosan-Based Hydrogels. *Polymers*, 15, 2482.
- [12] Z. Chen, J. Yao, J. Zhao, and S. Wang (2023). Injectable wound dressing based on carboxymethyl chitosan triple-network hydrogel for effective wound antibacterial and hemostasis. *Int. J. Biol. Macromol.*, 225, 1235–45.
- [13] X. Xu, Y. Zeng, Z. Chen, Y. Yu, H. Wang, X. Lu, J. Zhao, and S. Wang (2023). Chitosan-based multifunctional hydrogel for sequential wound inflammation elimination, infection inhibition, and wound healing. *Int. J. Biol. Macromol.*, 235, 123847.
- [14] J. Lu, X. Fan, J. Hu, J. Li, J. Rong, W. Wang, Y. Chen, W. Liu, J. Chen, and Y. Chen (2023). Construction and function of robust and moist bilayer chitosan-based hydrogel wound dressing. *Mater. Des.*, 226, 111604.
- [15] M. A. Gwak, S. J. Lee, D. Lee, S. A. Park, and W. H. Park (2023). Highly gallol-substituted, rapidly self-crosslinkable, and robust chitosan hydrogel for 3D bioprinting. *Int. J. Biol. Macromol.*, 227, 493–504.
- [16] T. K. Giri, A. Thakur, A. Alexander, Ajazuddin, H. Badwaik, and D. K. Tripathi (2012). Modified chitosan hydrogels as drug delivery and tissue engineering systems: present status and applications. *Acta Pharm. Sin. B*, 2, 439–49.
- [17] K. Thirupathi, C. J. Raorane, V. Ramkumar, S. Ulagesan, M. Santhamoorthy, V. Raj, G. S. Krishnakumar, T. T. V. Phan, and S-C. Kim (2023). Update on Chitosan-Based Hydrogels: Preparation, Characterization, and Its Antimicrobial and Antibiofilm Applications. *Gels*, 9, 35.
- [18] Y. Chen, J. Li, J. Lu, M. Ding, and Y. Chen (2022). Synthesis and properties of Poly(vinyl alcohol) hydrogels with high strength and toughness. *Polym. Test.*, 108, 107516.
- [19] K. Labus, L. Radosinski, and P. Kotowski (2021). Functional Properties of Two-Component Hydrogel Systems Based on Gelatin and Polyvinyl Alcohol—Experimental Studies Supported by Computational Analysis. *Int. J. Mol. Sci.*, 22.
- [20] H. Adelnia, R. Ensandoost, S. Shebbrin Moonshi, J. N. Gavvani, E. I. Vasafi, and H. T. Ta (2022). Freeze/thawed polyvinyl alcohol hydrogels: Present, past and future. *Eur. Polym. J.*, 164, 110974.
- [21] S. Liu, D. Li, Y. Wang, G. Zhou, K. Ge, and L. Jiang (2023). Adhesive, antibacterial and double crosslinked carboxylated polyvinyl alcohol/chitosan hydrogel to enhance dynamic skin wound healing. *Int. J. Biol. Macromol.*, 228, 744–53.
- [22] Ullah, A. A. Mamun, M. B. Zaidi, T. Roome, and A. Hasan (2023). A calcium peroxide incorporated oxygen releasing chitosan-PVA patch for Diabetic wound healing. *Biomed. Pharmacother.*, 165, 115156.
- [23] M. Hasnain, T. Kanwal, K. Rehman, S. R. U. Rehman, S. Aslam, T. Roome, S. Perveen, M. B. Zaidi, S. Saifullah, S. Yasmeen, A. Hasan, and M. R. Shah (2023). Microarray needles comprised of arginine-modified chitosan/PVA hydrogel for enhanced antibacterial and wound healing potential of curcumin. *Int. J. Biol. Macromol.*, 253, 126697.
- [24] H. Jafari and H. Namazi (2023). pH-sensitive biosystem based on laponite RD/chitosan/polyvinyl alcohol hydrogels for controlled delivery of curcumin to breast cancer cells. *Colloids Surf. B Biointerfaces*, 231, 113585.
- [25] H. Chopra, S. Bibi, S. Kumar, M. S. Khan, P. Kumar, and I. Singh (2022). Preparation and Evaluation of Chitosan/PVA Based Hydrogel Films Loaded with Honey for Wound Healing Application. *Gels*, 8, 111.
- [26] J. Sievers, K. Sperlich, T. Stahnke, C. Kreiner, T. Eickner, H. Martin, R. F. Guthoff, M. Schünemann, S. Bohn, and O. Stachs (2021). Determination of hydrogel swelling factors by two established and a

- novel non-contact continuous method. *J. Appl. Polym. Sci.*, 138, 50326.
- [27] K. Thongchai, P. Chuysinuan, T. Thanyacharoen, S. Techasakul, and S. Ummartyotin (2020). Characterization, release, and antioxidant activity of caffeic acid-loaded collagen and chitosan hydrogel composites. *J. Mater. Res. Technol.*, 9, 6512–20.
- [28] T. M. Tran Vo, T. Piroonpan, C. Preuksarattanawut, T. Kobayashi, and P. Potiyaraj (2022). Characterization of pH-responsive high molecular-weight chitosan/poly (vinyl alcohol) hydrogel prepared by gamma irradiation for localizing drug release. *Bioresour. Bioprocess.*, 9, 89.
- [29] T. Wang and S. Gunasekaran (2006). State of water in chitosan–PVA hydrogel. *J. Appl. Polym. Sci.*, 101, 3227–32.
- [30] F. Hemmatgir, N. Koupaei, and E. Poorazizi (2022). Characterization of a novel semi-interpenetrating hydrogel network fabricated by polyethylene glycol diacrylate/polyvinyl alcohol/tragacanth gum as a wound dressing. *Burns*, 48, 146–55.
- [31] H. Chopra, S. Bibi, Y. K. Mohanta, T. Kumar Mohanta, S. Kumar, I. Singh, P. R. Ranjan Rauta, A. Alshammari, M. Alharbi, and F. Alasmari (2023). In Vitro and In Silico Characterization of Curcumin-Loaded Chitosan–PVA Hydrogels: Antimicrobial and Potential Wound Healing Activity. *Gels*, 9, 394.
- [32] F. D. Martinez-Garcia, T. Fischer, A. Hayn, C. T. Mierke, J. K. Burgess, and M. C. Harmsen (2022). A Beginner's Guide to the Characterization of Hydrogel Microarchitecture for Cellular Applications. *Gels*, 8, 535.
- [33] Z. Chen, X. Yan, S. Yin, L. Liu, X. Liu, G. Zhao, W. Ma, W. Qi, Z. Ren, H. Liao, M. Liu, D. Cai, and H. Fang (2020). Influence of the pore size and porosity of selective laser melted Ti6Al4V ELI porous scaffold on cell proliferation, osteogenesis and bone ingrowth. *Mater. Sci. Eng. C*, 106, 110289.
- [34] F. Habibzadeh, S. M. Sadraei, R. Mansoori, N. P. Singh Chauhan, and G. Sargazi (2022). Nanomaterials supported by polymers for tissue engineering applications: A review. *Heliyon*, 8, e12193.
- [35] T. Ikeda, K. Ikeda, K. Yamamoto, H. Ishizaki, Y. Yoshizawa, K. Yanagiguchi, S. Yamada, and Y. Hayashi (2014). Fabrication and Characteristics of Chitosan Sponge as a Tissue Engineering Scaffold. *BioMed Res. Int.*, 2014, 786892.
- [36] J. Grenier, H. Duval, P. Lv, F. Barou, C. Le Guilcher, R. Aid, B. David, and D. Letourneur (2022). Interplay between crosslinking and ice nucleation controls the porous structure of freeze-dried hydrogel scaffolds. *Biomater. Adv.*, 139, 212973.
- [37] Y. Zhang, M. Jiang, Y. Zhang, Q. Cao, X. Wang, Y. Han, G. Sun, Y. Li, and J. Zhou (2019). Novel lignin–chitosan–PVA composite hydrogel for wound dressing. *Mater. Sci. Eng. C*, 104, 110002.
- [38] Z. I. Abdeen, A. F. El Faragy, and N. A. Negrn (2018). Nanocomposite framework of chitosan/polyvinyl alcohol/ZnO: Preparation, characterization, swelling and antimicrobial evaluation. *J. Mol. Liq.*, 250, 335–43.
- [39] D. Mukherjee, M. Azamthulla, S. Santhosh, G. Dath, A. Ghosh, R. Natholia, J. Anbu, B. V. Teja, and K. M. Muzammil (2018). Development and characterization of chitosan-based hydrogels as wound dressing materials. *J. Drug Deliv. Sci. Technol.*, 46, 498–510.
- [40] R. Gobi and R. S. Babu (2023). In-vitro study on chitosan/PVA incorporated with nickel oxide nanoparticles for wound healing application. *Mater. Today Commun.*, 34, 105154.
- [41] S. Bi, P. Wang, S. Hu, S. Li, J. Pang, Z. Zhou, G. Sun, L. Huang, X. Cheng, S. Xing, and X. Chen (2019). Construction of physical-crosslink chitosan/PVA double-network hydrogel with surface mineralization for bone repair. *Carbohydr. Polym.*, 224, 115176.
- [42] S. Bi, J. Pang, L. Huang, M. Sun, X. Cheng, and X. Chen (2020). The toughness chitosan–PVA double network hydrogel based on alkali solution system and hydrogen bonding for tissue engineering applications. *Int. J. Biol. Macromol.*, 146, 99–109.
- [43] D. M. Suflet, I. M. Popescu, I. M. Pelin, D. L. Ichim, O. M. Daraba, M. Constantin, and G. Fundeanu (2021). Dual Cross-Linked Chitosan/PVA Hydrogels Containing Silver Nanoparticles with Antimicrobial Properties. *Pharmaceutics*, 13, 1461.
- [44] S. Bhatt, G. Thakur, and M. Nune (2023). Preparation and characterization of PVA/Chitosan cross-linked 3D scaffolds for liver tissue engineering. *Mater. Today Proc.*, S2214785323007952.
- [45] Ehterami, M. Salehi, S. Farzamfar, H. Samadian, A. Vaez, H. Sahrpeyma, and S. Ghorbani (2020). A promising wound dressing based on alginate hydrogels containing vitamin D3 cross-linked by calcium carbonate/d-glucono- δ -lactone. *Biomed. Eng. Lett.*, 10, 309–19.
- [46] M. Zhang, G. Wang, X. Zhang, Y. Zheng, S. Lee, D. Wang, and Y. Yang (2021). Polyvinyl Alcohol/Chitosan and Polyvinyl Alcohol/Ag@MOF Bilayer Hydrogel for Tissue Engineering Applications. *Polymers*, 13, 3151.